JEM

SUPPLEMENTAL MATERIAL

Sultana et al. http://www.jem.org/cgi/content/full/jem.20100276/DC1

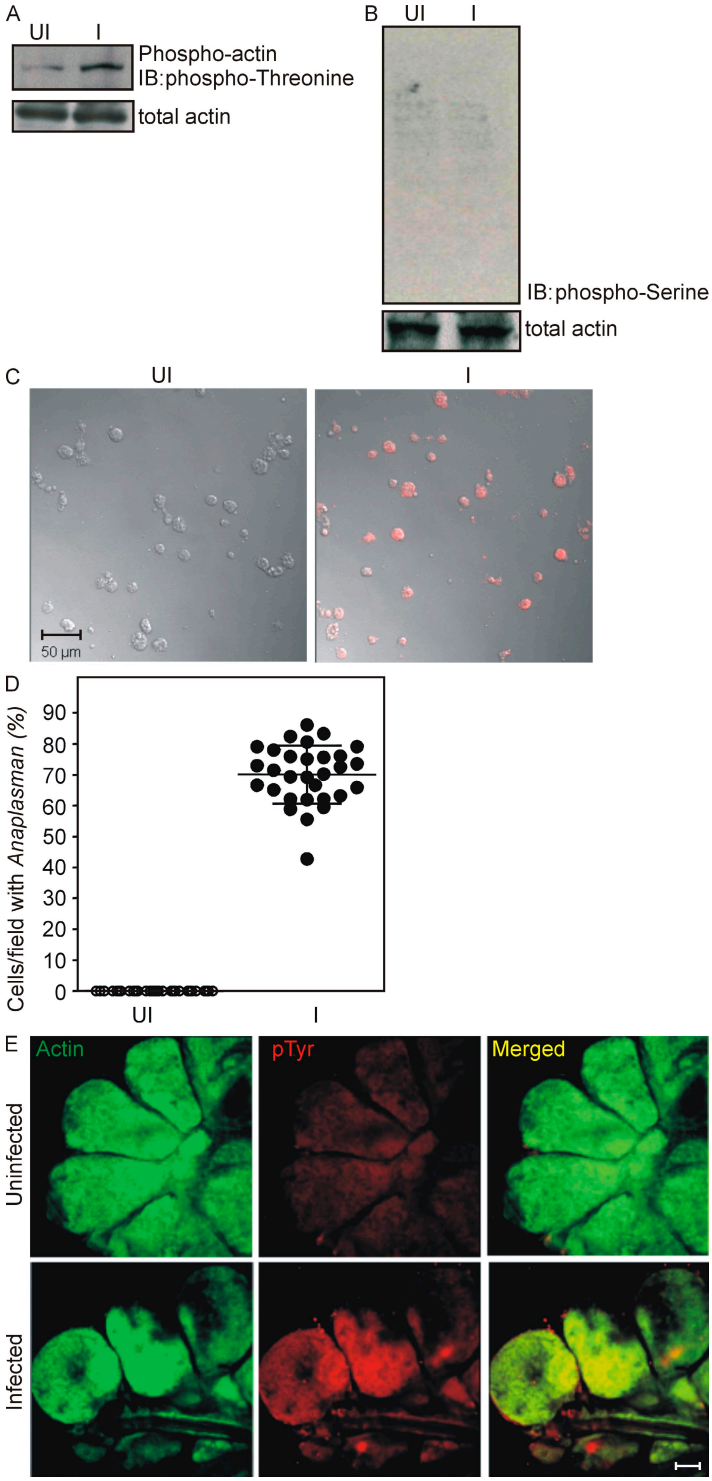

Figure S1. ***A. phagocytophilum*** **induces both phosphothreonine and phosphotyrosine phosphorylation of actin in** ***I. scapularis.*** Tick lysates with (I) or without (UI) *A. phagocytophilum* were probed with antibodies specific against phospho-threonine (A) or with phospho-serine (B) to determine the threonine/serine phosphorylation of actin. Total actin levels served as the loading control. Representative data are shown from three independent experiments. (C) Immunofluorescence images of uninfected (UI) and *A. phagocytophilum*–infected (I) tick cells at 48 h after infection were stained for *A. phagocytophilum*. Bar, 50 µM. Representative images are shown from three independent experiments. (D) Quantification of the percentage of *A. phagocytophilum*–infected cells/microscopic field was determined from 25 random fields to total number of cells in each field. Error bars show mean ± SD. (E) Phosphorylation of actin in unfed tick salivary glands. Immunofluorescence of unfed tick salivary glands with (I) or without (UI), *A. phagocytophilum* was probed against total actin (green) and pTyr (red). Representative images from three independent experiments are shown. Bar, 20 µM.

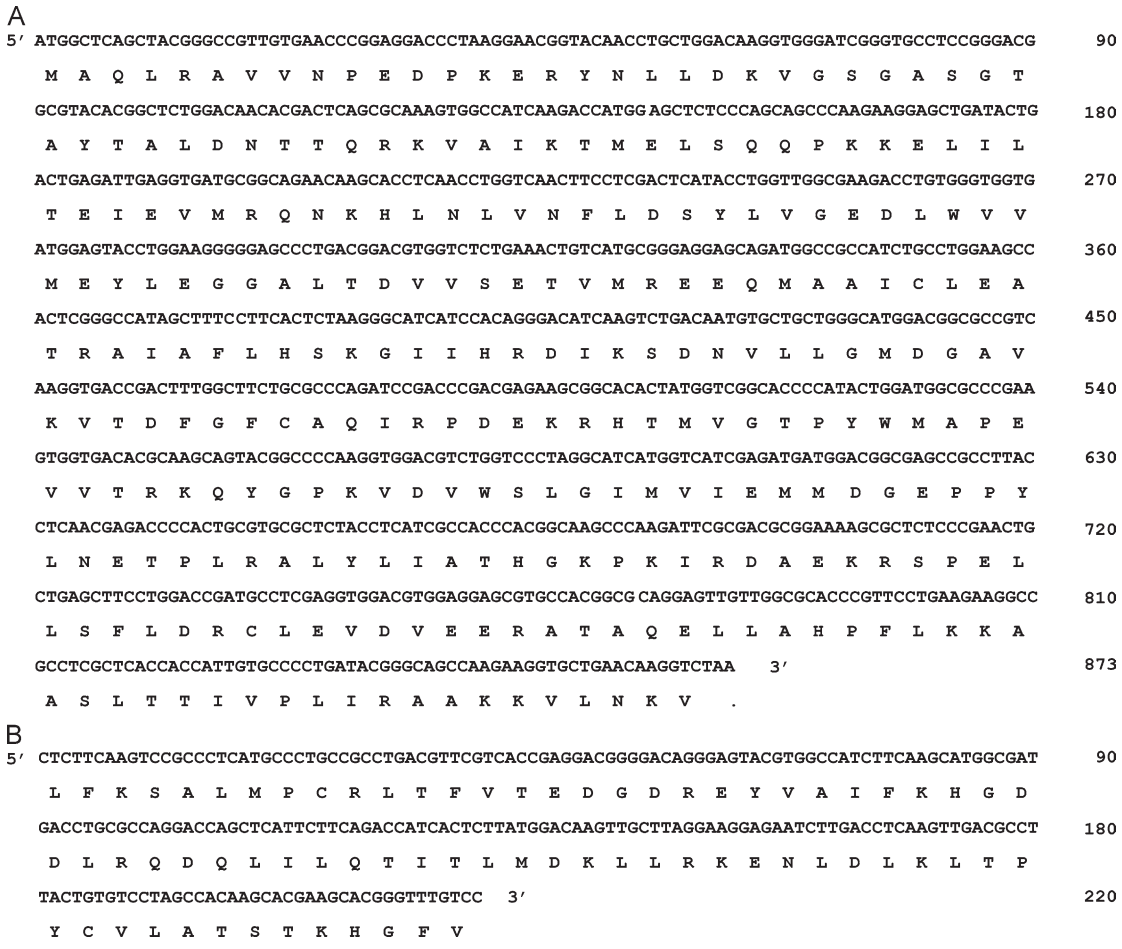

Figure S2. *Ixodes* PAK1 and PI3K sequences. Nucleotide and deduced amino acid sequences (partial) of *ipak1* (A) and *ipi3k* (B) are shown. The *ipak1* and *ipi3k* genes were cloned into a pGEMT-easy vector and sequenced from both ends. The resulted sequences were aligned using SeqMan software, analyzed, and translated using SeqBuilder software (DNASTAR, Inc.). Oligonucleotides for the amplification of *ipak1* and *ipi3k* genes were designed based on the EST sequences obtained from the *I. scapularis* genome database.

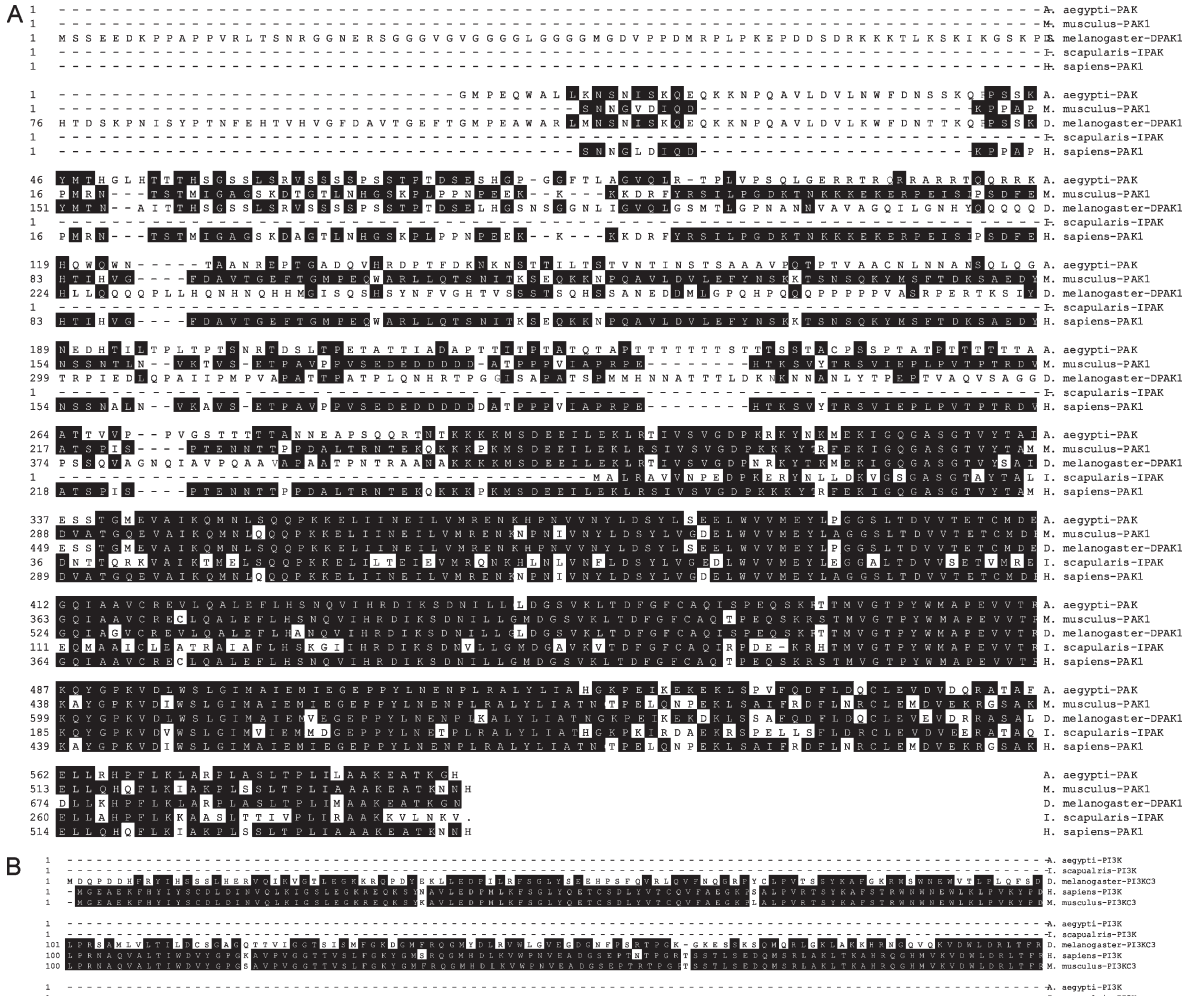

Figure S3. Alignments of *Ixodes* PAK1 and PI3K sequences. (A) ClustalW alignment of deduced amino acid sequences of *Ixodes* PAK1 (partial sequences) with PAK1 sequences from *H. sapiens* (accession no. NP_002567), *M. musculus* (accession no. NP_035165), *A. aegypti* (accession no. XP_001655678), and *D. melanogaster* (accession no. AAB01209) with 82.6/65.9, 82.6/65.6, 84/69, and 82.2/64.8% similarity/identity, respectively. (B) ClustalW alignment of deduced amino acid sequences of IPI3K (partial sequences) with *H. sapiens* PI3K (accession no. CAA87094), *M. musculus* PI3KC3 (accession no. NP_852079), *A. aegypti* (accession no. XP_001660421), and *D. melanogaster* (accession no. NP_477133) with 87.7/82.2, 87.7/82.2, 90.4/83.6, and 87.7/82.2% similarity/identity, respectively. Accession numbers are reference sequence numbers from NCBI Protein database.

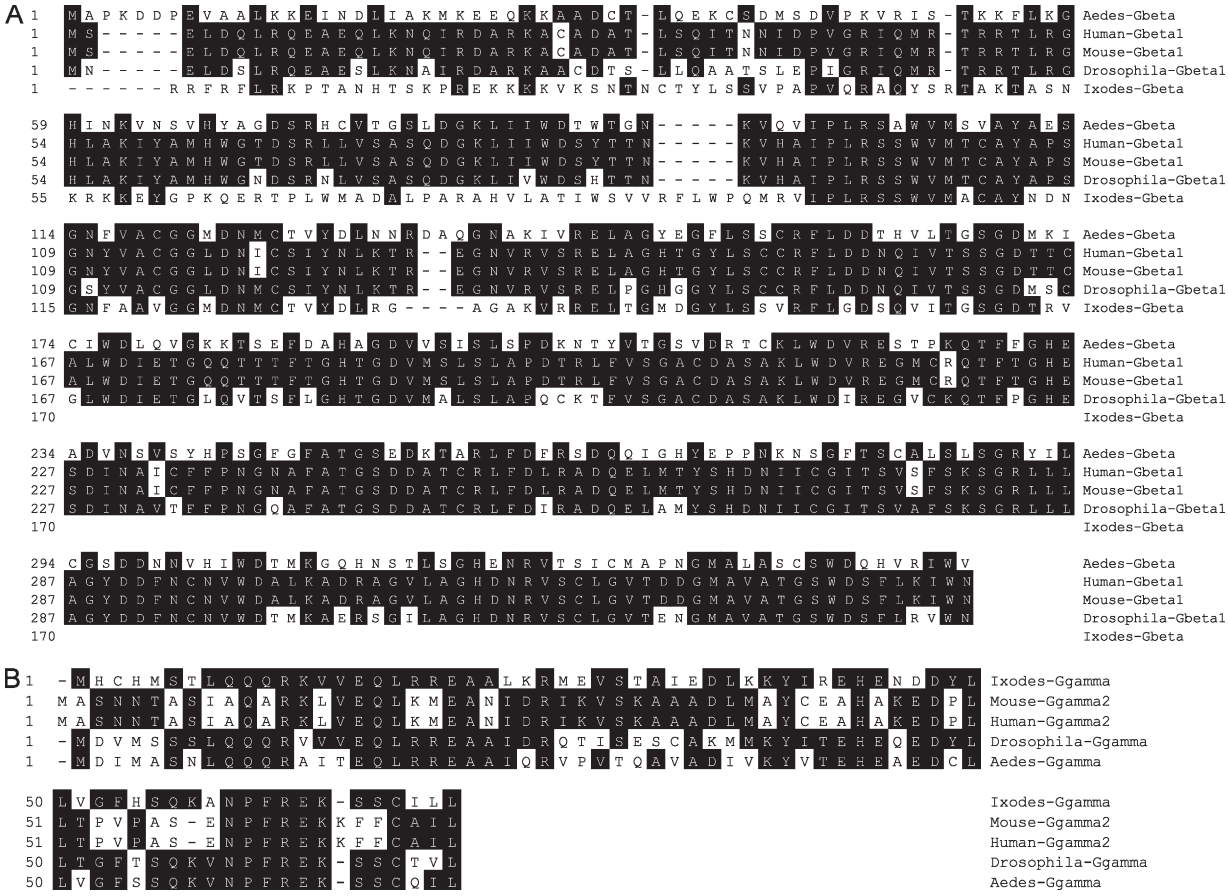

Figure S4. Alignments of *Ixodes* Gβγ subunit sequences. (A) ClustalW alignment of partial deduced amino acid sequences of *Ixodes* G protein β subunit (accession no. XP_002401352) with sequences from *H. sapiens* (accession no. NP_002065), *M. musculus* (accession no. NP_001153488), *A. aegypti* (accession no. XP_001653114), and *D. melanogaster* (accession no. P26308) with 55.1, 55.3, 58.8, and 54.7% identity, respectively. (B) ClustalW alignment of deduced amino acid sequences of *Ixodes* G-protein γ subunit (EEC12500) with *H. sapiens* (accession no. NP_444292), *M. musculus* (accession no. NP_001033726), *A. aegypti* (accession no. XP_001661584), and *D. melanogaster* (accession no. NP_724718) shows 44.1, 44.1, 64.6, and 66.2% identity, respectively. Accession numbers are reference sequence numbers from NCBI Protein database.

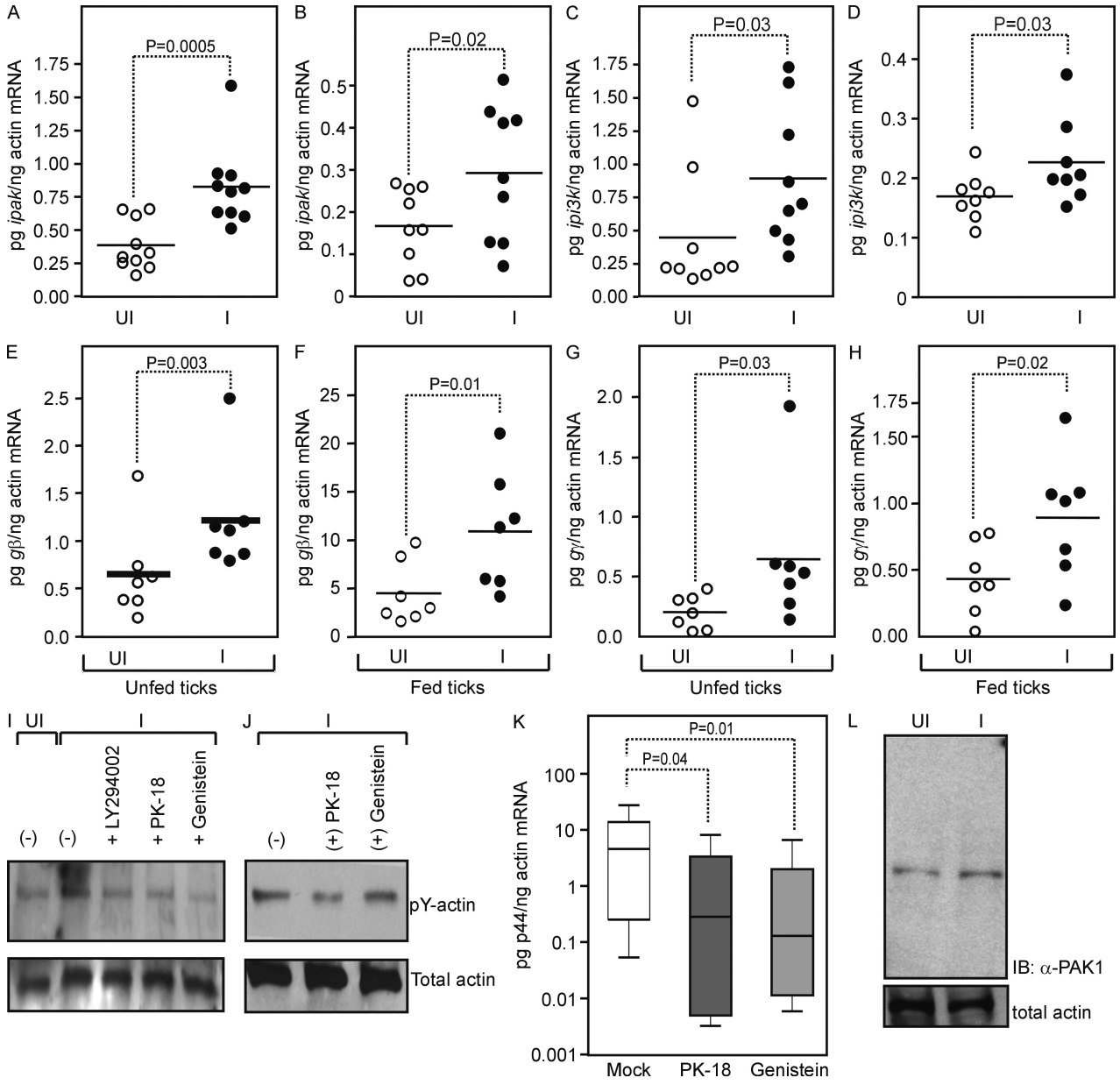

Figure S5. Expression and inhibition of *I. scapularis* PAK1, PI3K, Gβ, Gγ, or tyrosine kinases in ticks. Q-RT-PCR results from 7–10 individual uninfected (UI) and *A. phagocytophilum*–infected (I) unfed ticks (A, C, E, and G) and 48-h fed ticks (B, D, F, and H). Fed ticks were generated as described in Materials and methods. Expression levels of *ipak1* (A and B), *ipi3k* (C and D), *igβ* (E and F), and *igγ* (G and H) in *A. phagocytophilum*–infected (I) unfed or fed ticks in comparison to uninfected controls (UI). The levels of *ipak1*, *ipi3k*, *igβ*, and *igγ* transcripts were normalized against tick *β-actin* mRNA. Horizontal bars in A–H indicate mean values of the data points. (I) Immunoblot of unfed uninfected (UI) or *A. phagocytophilum*–infected (I) ticks were injected with mock (−), LY294002 (PI3K inhibitor), PK-18 (potent PAK1 inhibitor), or Genistein (protein tyrosine kinase inhibitor). (J) Immunoblot showing the levels of phosphorylated and total actin during *A. phagocytophilum* acquisition by mock (DMSO), PK-18, and Genistein-injected ticks. Phosphorylated actin (pY-actin) levels were analyzed by probing with pTyr antibody. Total actin served as loading control. (K) Q-RT-PCR showing *A. phagocytophilum* burden in inhibitor-injected ticks and the mock (DMSO) control. *A. phagocytophilum* burden was measured by quantifying *p44* mRNA levels and normalized against tick *β-actin* mRNA. Statistics were performed using the Student's *t* test and the p-value is shown. Error bars show mean ± SD. (L) Immunoblot showing *I. scapularis* PAK1 specific cross-reactivity with mammalian PAK1 antibody. Total actin served as loading control. Two independent experiments yielded similar results in all panels.

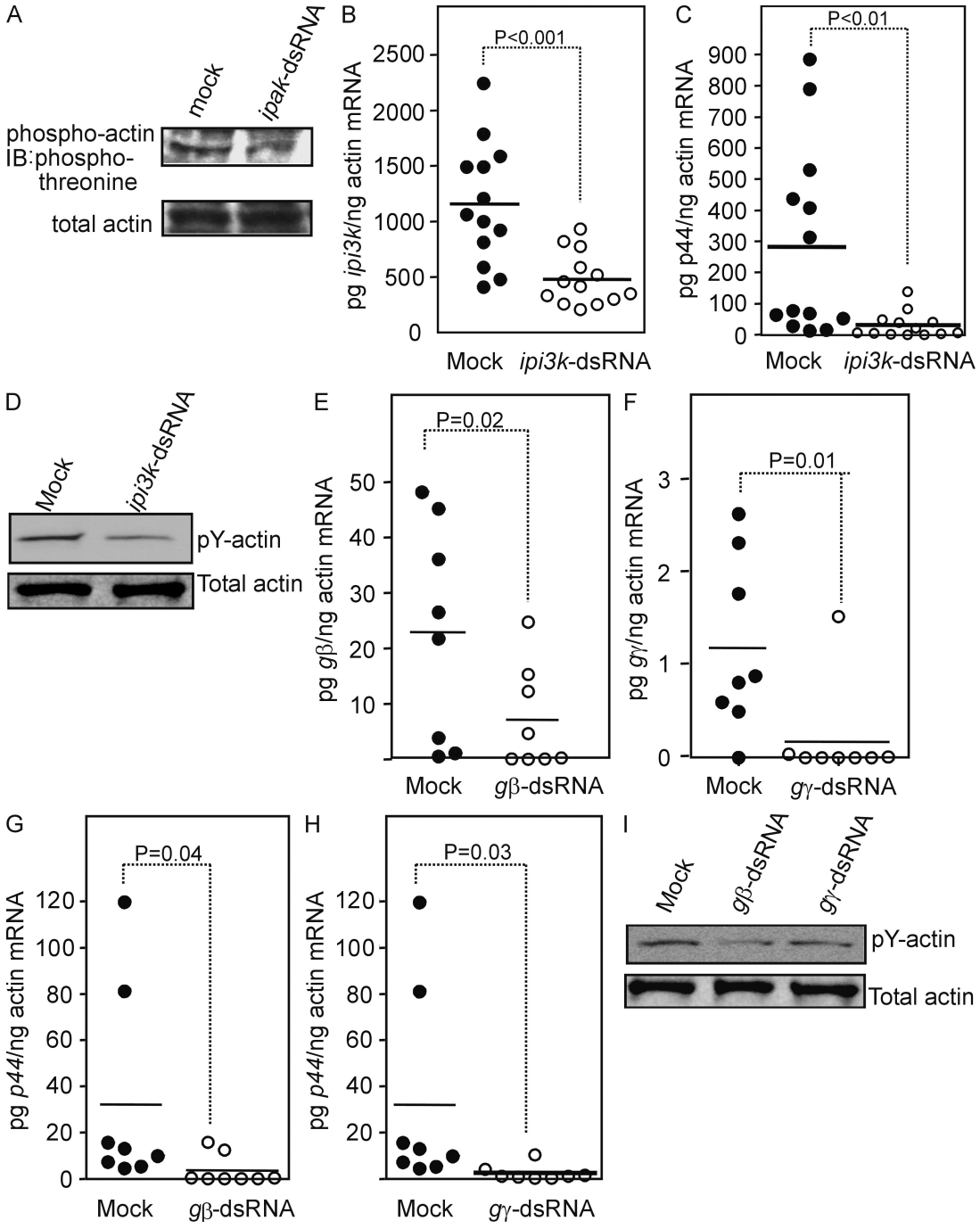

Figure S6. Silencing of *ipak*, *ipi3k*, *gβ*, and *gγ* reduces actin phosphorylation in *I. scapularis*. (A) Silencing of *ipak* showing threonine phosphorylation of actin. Mock and *ipak*-dsRNA–injected tick lysates (from 48 h during feeding ticks) were probed with phospho-threonine antibody. Total actin serves as loading control. Silencing of *ipi3k*, *igβ*, or *igγ* affects the *A. phagocytophilum* burden and actin phosphorylation in ticks during acquisition. Q-RT-PCR results showing the knockdown efficiency of *ipi3k* (B), *igβ* (E), and *igγ* (F) in mock (buffer alone) and *ipi3k*-, *igβ*-, or *igγ*-silenced ticks from 48 h during feeding. The mRNA levels of *ipi3k* (B), *igβ* (E), and *igγ* (F) in silenced and mock control ticks were compared. *A. phagocytophilum* burden was measured by quantifying *p44* levels in *ipi3k*- (C), *igβ*- (G), or *igγ* (H)-silenced ticks during acquisition from mouse host. Immunoblots of phosphorylated actin (detected by phosphotyrosine-specific antibody) in *ipi3k*-silenced (D) or *igβ*- or *igγ*-silenced (I) ticks and mock controls. Two independent experiments yielded similar results. Total actin levels probed with actin antibody served as the loading control. Horizontal bars in B, C, and E–H indicate mean values of the data points.

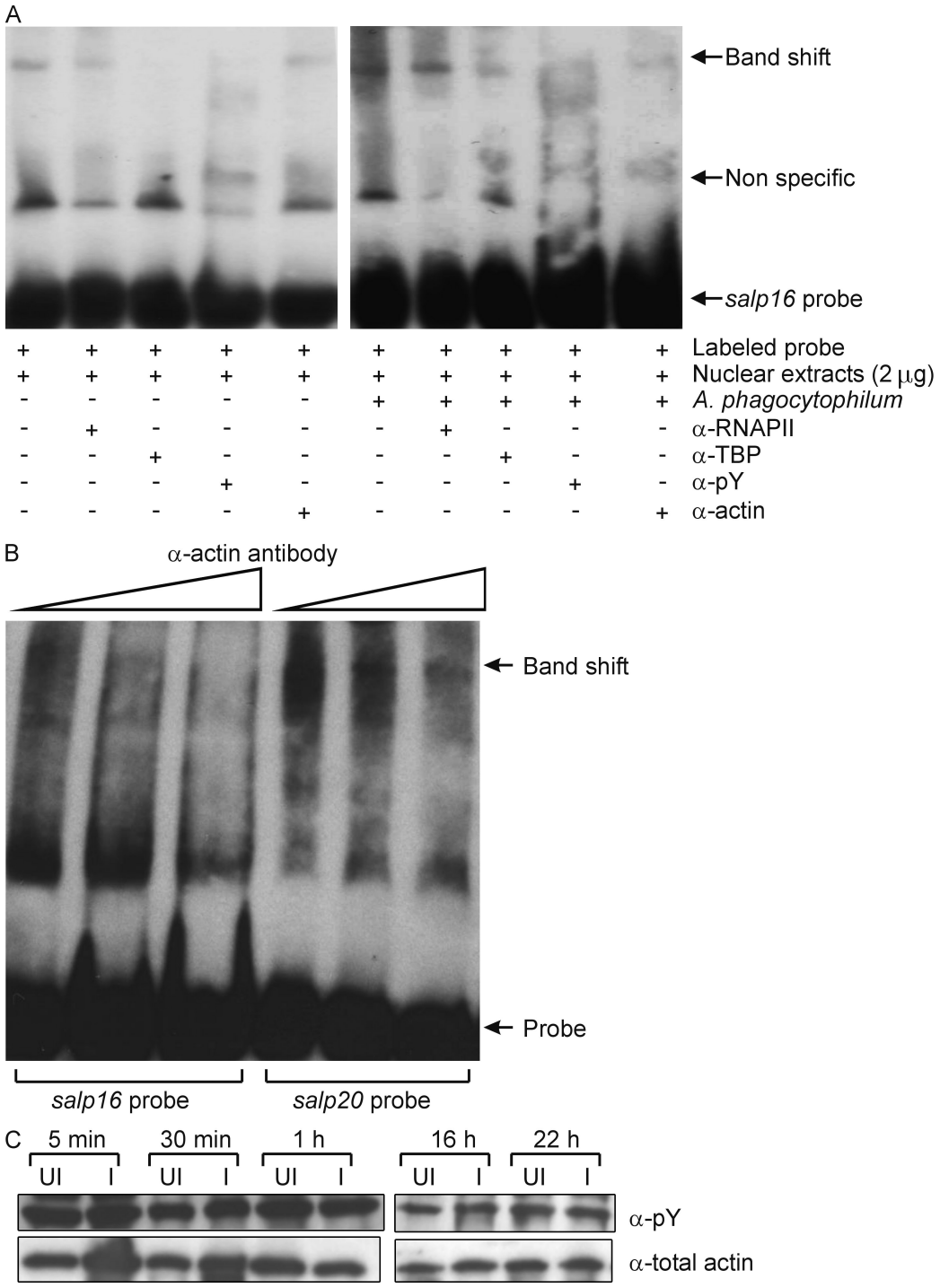

Figure S7. Antibodies against phosphotyrosine, actin, RNAPII, and TBP blocked the band shift with *salp16* probe. (A) EMSA performed with antibodies against RNAPII, TBP, phosphotyrosine, or actin showing *salp16* band shifts with nuclear extract proteins from uninfected or *A. phagocytophilum*–infected ticks collected at 48-h engorgement. 2 µg of nuclear extracts (in all lanes) were treated with respective antibodies against RNAPII, TBP, phosphotyrosine, and actin. No antibody samples served as control. Band shift and labeled probes are denoted with arrows. (B) EMSA performed with 2 µg of nuclear extracts from *A. phagocytophilum*–infected ticks (in all lanes) and antibody against actin in three different increasing concentrations (1, 2, and 3 µg) showing the band shift with *salp16* and *salp20* probes. Representative data from three independent experiments is shown. Band shift and labeled probes are denoted with arrows. (C) Primary cultures of human neutrophils were isolated from healthy donor and infected with *A. phagocytophilum* as mentioned in experimental procedures. Lysates infected (I) or not (UI) with *A. phagocytophilum* at different time points (5 and 30 min and 1, 16, and 22 h) were assessed for actin phosphorylation. Representative data from two independent experiments is shown. The phosphorylated actin (pY-actin) was detected by probing with pTyr-specific and total actin with actin-specific antibodies, respectively.

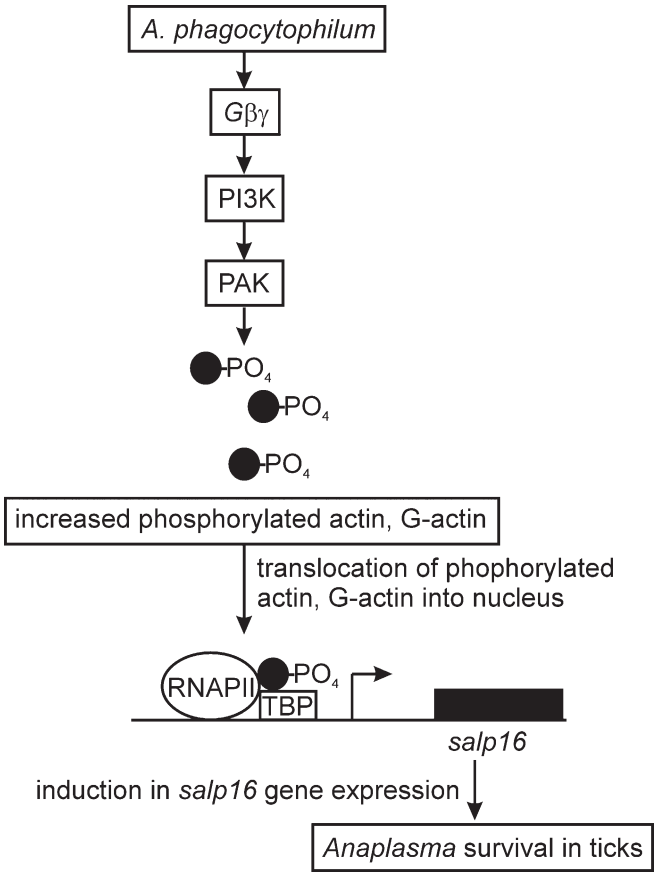

Figure S8. Model depicting *A. phagocytophilum*–induced actin phosphorylation in the context of *Ixodes* PI3K–PAK1 signaling, which selectively regulates *salp16* gene transcription. *A. phagocytophilum* stimulates the G protein βγ subunits to activate PI3K and PAK1 signal transduction pathways that lead to the induction in phosphorylated actin. Phosphorylation of actin inhibits actin filament nucleation and elongation, leading to a reduction in actin polymerization. Black circles represent actin monomers. Increased G-actin monomers translocate to the cell nuclei and associates with TBP and RNAPII to selectively regulate *salp16* gene expression, a gene required for *A. phagocytophilum* survival in ticks.

Table S1.Q4 Quantification of Western blots shown in this study

Figure[a]	Panel[b]	Sample[c]	Relative intensity[d]	Fold difference[e]
Fig. 1	B	UI	0.18933519	4.58
Fig. 1	B	I	0.86791879	4.58
Fig. 1	C	UI	0.284730313	2.80
Fig. 1	C	I	0.79738387	2.80
Fig. 1	D	UI (−) 8h	0.133444051	1.01
Fig. 1	D	UI (+) 8h	0.119188797	1.01
Fig. 1	D	I (−) 8h	0.135124095	1.01
Fig. 1	D	I (+) 8h	0.120108129	1.01
Fig. 1	D	UI (−) 24h	0.174460693	2.89
Fig. 1	D	UI (+) 24h	0.179763132	3.41
Fig. 1	D	I (−) 24h	0.504930168	2.89
Fig. 1	D	I (+) 24h	0.613331705	3.41
Fig. 1	D	UI (−) 48h	0.165301135	6.40
Fig. 1	D	UI (+) 48h	0.206225901	4.13
Fig. 1	D	I (−) 48h	1.058397547	6.40
Fig. 1	D	I (+) 48h	0.851410414	4.13
Fig. 1	D	UI (−) 7 d	0.240928047	5.40
Fig. 1	D	UI (+) 7 d	0.347082894	3.53
Fig. 1	D	I (−) 7 d	1.30041193	5.40
Fig. 1	D	I (+) 7 d	1.225975341	3.53
Fig. 1	D	UI (−) 10 d	0.268633688	4.51
Fig. 1	D	UI (+) 10 d	0.268813361	4.27
Fig. 1	D	I (−) 10 d	1.210262117	4.51
Fig. 1	D	I (+) 10 d	1.148910458	4.27
Fig. 1	F	UI	0.075603978	3.50
Fig. 1	F	I	0.256608651	3.50
Fig. 1	G	UI	0.927120655	2.33
Fig. 1	G	I	2.158783009	2.33
Fig. 1	H	UI/	0.298895208	4.74
Fig. 1	H	I	1.416359386	4.74
Fig. 1	I	UI	1.355566452	2.57
Fig. 1	I	I	3.477576411	2.57
Fig. 2	A	A. phag. 24 h	0.317391637	
Fig. 2	A	A. phag+ Genistein 24 h	0.279181483	1.14
Fig. 2	A	A. phag+ PK-18 24 h	0.164958301	1.92
Fig. 2	A	A. phag+ LY294002 24 h	0.271695993	1.17
Fig. 2	A	A. phag. 48 h	0.316142901	
Fig. 2	A	A. phag+ Genistein 48 h	0.149414449	2.12
Fig. 2	A	A. phag+ PK-18 48 h	0.113826564	2.78
Fig. 2	A	A. phag+ LY294002 48 h	0.155920259	2.03
Fig. 2	A	A. phag. 72 h	0.176454617	
Fig. 2	A	A. phag+ Genistein 72 h	0.087455765	2.02
Fig. 2	A	A. phag+ PK-18 72 h	0.075190078	2.35
Fig. 2	A	A. phag+ LY294002 72 h	0.026190171	6.74
Fig. 2	C	UI after IP	0.2226104	4.83
Fig. 2	C	I after IP	1.074467324	4.83
Fig. 2	E	Mock	0.507994571	3.71
Fig. 2	E	ipak-dsRNA	0.136853772	3.71
Fig. 3	A	UI-lane1	0.472361094	1.23
Fig. 3	A	UI-lane2	0.535839252	1.85
Fig. 3	A	UI-lane3	0.664769852	2.11

Table S1.Q4 Quantification of Western blots shown in this study *(Continued)*

Figure[a]	Panel[b]	Sample[c]	Relative intensity[d]	Fold difference[e]
Fig. 3	A	I-lane1	0.578857326	1.23
Fig. 3	A	I-lane2	0.993219965	1.85
Fig. 3	A	I-lane3	1.40408263	2.11
Fig. 3	C	Mock-lane1	0.624543806	5.03
Fig. 3	C	Mock-lane2	0.79174329	6.79
Fig. 3	C	Mock-lane3	0.944938347	4.33
Fig. 3	C	ipi3k-dsRNA-lane1	0.124189668	5.03
Fig. 3	C	ipi3k-dsRNA-lane2	0.116519453	6.79
Fig. 3	C	ipi3k-dsRNA-lane3	0.218419321	4.33
Fig. 3	D	Mock-lane1	0.419622595	
Fig. 3	D	Mock-lane2	0.733205602	
Fig. 3	D	Mock-lane3	1.011406211	
Fig. 3	D	gbeta-dsRNA-lane1	0.218057265	1.92
Fig. 3	D	gbeta-dsRNA-lane2	0.373495166	3.36
Fig. 3	D	gbeta-dsRNA-lane3	0.296807546	3.41
Fig. 3	D	ggamma-dsRNA-lane1	0.103262917	4.06
Fig. 3	D	ggamma-dsRNA-lane2	0.206713562	3.55
Fig. 3	D	ggamma-dsRNA-lane3	0.242992441	4.16
Fig. 3	F	UI-activated RAC1	0.54845103	1.03
Fig. 3	F	I-activated RAC1	0.534650334	1.03
Fig. 3	F	UI-activated CDC42	0.420756472	1.07
Fig. 3	F	I-activated CDC42	0.449237915	1.07
Fig. 4	A	UI-G-actin	0.610096951	2.19
Fig. 4	A	I-G-actin	1.33800392	2.19
Fig. 4	A	UI-F-actin	0.93806741	2.88
Fig. 4	A	I-F-actin	0.326277044	2.88
Fig. 5	A	UI-TBP	1.22847488	1.06
Fig. 5	A	I-TBP	1.156029471	1.06
Fig. 5	A	UI-G-actin	0.604121649	2.05
Fig. 5	A	I-G-actin	1.237706857	2.05
Fig. 5	A	UI-pY-actin	1.012806722	2.29
Fig. 5	A	I-pY-actin	2.320901683	2.29
Fig. 5	A	UI-TBP (IP:RNAPII)	0.532530754	3.23
Fig. 5	A	I-TBP (IP: RNAPII)	1.720029474	3.23
Fig. 8	A	Mock-pY actin	0.34110067	12.11
Fig. 8	A	ipak-dsRNA-pY actin	0.080563457	12.11
Fig. 8	A	Mock-TBP	0.911456714	1.14
Fig. 8	A	ipak-TBP	0.796072422	1.14
Fig. 8	A	Mock-RNAPII	0.542584822	1.03
Fig. 8	A	ipak-RNAPII	0.528794681	1.03
Fig. 8	C	salp16-pY actin	0.491705513	6.38
Fig. 8	C	salp20-pY actin	0.077105395	6.38
Fig. 8	C	salp16-TBP	0.316275132	1.43
Fig. 8	C	salp20-TBP	0.221212208	1.43
Fig. 8	C	salp16-RNAPII	0.47846953	1.22
Fig. 8	C	salp20-RNAPII	0.390809181	1.22
Fig. S1	A	UI	0.210914204	2.60
Fig. S1	A	I	0.547530204	2.60
Fig. S5	I	UI (−)	0.219998481	ND
Fig. S5	I	I (−)	0.66540911	
Fig. S5	I	I + LY294002	0.178474486	3.73
Fig. S5	I	I + PK-18	0.083908515	7.93
Fig. S5	I	I + Genistein	0.020408722	32.60

Table S1.Q4 Quantification of Western blots shown in this study *(Continued)*

Figure[a]	Panel[b]	Sample[c]	Relative intensity[d]	Fold difference[e]
Fig. S5	J	I (−)	0.242963442	
Fig. S5	J	I + PK-18	0.037999338	6.39
Fig. S5	J	I + Genistein	0.103762854	2.34
Fig. S5	L	UI	0.12426126	3.07
Fig. S5	L	I	0.381340735	3.07
Fig. S6	A	Mock	0.902465844	2.67
Fig. S6	A	*ipak*-dsRNA-phospho-Threonine	0.337029076	2.67
Fig. S6	D	Mock-pY actin	0.220870162	3.16
Fig. S6	D	ipi3k-dsRNA-pY-actin	0.06999562	3.16
Fig. S6	I	mock-pY actin	0.26952826	
Fig. S6	I	G-beta-dsRNA-pY actin	0.106537504	2.53
Fig. S6	I	G-gamma-dsRNA-pY actin	0.111021138	2.43

[a]Numbers correspond to Figure numbers in the manuscript
[b]Panel letters correspond to figure panels in the manuscript
[c]Names correspond to sample names shown in the Figures
[d]Relative intensity is calculated as mentioned in Materials and methods and was used to calculate fold differences
[e]Fold difference is calculated between uninfected (UI) and infected (I) samples, mock and dsRNA-treated samples, or untreated (−) and inhibitor-treated (+) samples. Fold difference in Western blots performed after DNA precipitation is calculated between *salp16* and *salp20* samples.